

FLIGHT EVALUATION OF ADAPTIVE HIGH-BANDWIDTH CONTROL METHODS FOR UNMANNED HELICOPTERS

J. Eric Corban *

Guided Systems Technologies, Inc., P.O. Box 1453, McDonough, GA 30253

Anthony J. Calise,[†] J. V. R. Prasad,[‡] Jeong Hur,^{††} and Nakwan Kim ^{‡‡}

Georgia Institute of Technology, School of Aerospace Engineering, Atlanta, GA 30332-0150

Abstract

This paper summarizes design of a high-bandwidth nonlinear adaptive attitude command system for an unmanned helicopter test bed, and presents an evaluation of the controller in both nonlinear simulation and flight test. The attitude command system features a dynamic inversion control law augmented by an on-line neural network. The design is cast in an output feedback setting. The inverting control law is based on a simple linear model of the helicopter and its actuators at the hover condition. An error observer-based method for output feedback design uses either a proportional plus derivative, or a proportional, integral and derivative form for the linear compensator. Pseudo control hedging is employed to prevent adaptation to input characteristics such as actuator position and rate saturation. A brief description is given of the unmanned helicopter testbed, real-time control system implementation, simulation, and flight test facilities. Stable adaptation for a design natural frequency up to 9 radians per second is flight demonstrated in the presence of actuator and unmodeled control rotor dynamics, system time delays, sensor noise, sensor latency, gusts and input saturation.

Introduction

Use of large numbers of small, unmanned air vehicles is envisioned on future battlefields. However, a high degree of autonomy will be required to realize the full potential of these small vehicles. In particular, they may be required to autonomously navigate amongst the obstacles typical of an urban environment. The combination of their small size and mass, resultant sensitivity to atmospheric turbulence and gusts, and a

limited ability to “see” beyond the closest obstacles will necessitate a *high-bandwidth* control solution.

Note that a skilled human pilot of a small remotely-controlled flight vehicle (e.g. hobby aircraft) is able to anticipate and interact with high frequency dynamics and system delays, thus achieving a very high effective bandwidth. However, both classical and modern control design methods are fundamentally limited by the presence of unmodeled high frequency effects, as are traditional applications of adaptive control. This limits autopilot bandwidth, which in turn limits the maneuvering capability of the aircraft while under automatic control. However, recent extensions of neural network-based nonlinear adaptive control to include output feedback presents the opportunity to explicitly account for and adapt to unmodeled and potentially nonlinear dynamics.

While adaptation can now be used to overcome both parametric uncertainty and unmodeled dynamics, it is not able to tolerate the actuator position and rate saturation that naturally occurs at the edge of the maneuvering flight envelop. This problem feature can be successfully addressed using a method known as pseudo control hedging^{2,3}. In effect, the command filter is modified to prevent the adaptation law from “seeing” and adapting to input characteristics such as position and rate saturation. The combination of these two design improvements (i.e. output feedback and pseudo control hedging) to the original state-feedback adaptive autopilot design presented by the authors in Reference 1 enables high-bandwidth adaptive operation all the way out to the limits of the aircraft’s maneuvering envelop.

Adaptive methods can also reduce control system design dependence on high-fidelity modeling, and offer a means for rapid and affordable transition of developed control system technology from one platform variant to another. This paper reports on a current flight test program directed at evaluation of new methods for design of high-bandwidth adaptive flight control systems for small unmanned rotorcraft. We begin in the next section with an overview of neural

* President, Member AIAA

† Professor, Fellow AIAA

‡ Professor, Member AIAA

†† Research Engineer

‡‡ Graduate Student

network adaptive state feedback control. This is followed by a summary of previously reported adaptive output feedback designs and the method of pseudo control hedging. This is followed by a section which presents an overview of the unmanned helicopter simulation and flight test facility used to generate numerical results. The paper concludes with the presentation of recent flight test and nonlinear simulation results which document the performance achieved to date using the referenced high-bandwidth adaptive designs.

Adaptive Attitude Command System

State Feedback Formulation

An adaptive attitude command system for unmanned helicopters that employed a state feedback formulation was previously reported¹. State feedback pertains to applications in which the entire state of a system is sensed and available to the feedback control process. In reference 1, an approximate linear model of the rotational dynamics of the helicopter was inverted at a nominal operating condition. An artificial neural network was employed on-line to cancel the error that results from the use of an inexact model of the plant for inversion.

Small helicopters typically employ a mechanical and aerodynamic system (sometimes referred to as a control rotor) to alter its flight characteristics. This is done so that a human can better manage the piloting task. Although this mechanical feedback system can be a hindrance in the design of automatic flight controls, it is desirable to retain this feature on a research test bed to allow for reasonable handling qualities during open loop flight operations. The state feedback design of Reference 1 ignored both control rotor dynamics and actuator dynamics.

Good performance of the state feedback adaptive system was obtained in both simulation and flight test¹, and clearly demonstrated the benefits of on-line adaptation. These benefits include: (1) nonlinear control design without the need for gain scheduling, (2) real time adaptation to uncertain nonlinear effects, (3) the ability to adapt to overcome parametric uncertainty. In this context, parametric uncertainty refers to the case in which a model describing the dynamics of a plant is erroneous due to uncertain coefficients that appear in the dynamic equations. These uncertainties may be due to modeling error, or may come about when a failure occurs. This is different from uncertainty due to unmodeled dynamics, which corresponds to the situation in which the dimension of the plant model is

lower than the dimension of the actual plant dynamics. Flight test revealed that the state-feedback controller bandwidth was limited to 2-3 radians per second by the unmodeled control rotor and actuator dynamics of the test bed helicopter, and time delays resulting from practical digital implementation of the control.

Output Feedback Formulation

In References 2 and 3, the authors presented a direct output feedback approach to design of an attitude command system for an unmanned helicopter test bed. Output feedback concerns the situation in which only a subset of the total state vector, or a function of the state vector, is available for feedback. The term "direct" in this context refers to an output feedback control architecture that avoids the use of a state observer.

More recently, an alternate output feedback architecture was reported that falls between the direct approach and other existing approaches that rely on the use of a state observer. This approach is referred to as *Observing the Tracking Error Dynamics*. The role of the observer in this setting is to construct an error vector whose elements consist of estimates of the tracking error and its time derivatives up to and including the $(r-1)$ time derivative, where r is the relative degree of the regulated output of the system to be controlled. As in the direct approach previously mentioned, this method is not restricted by the relative degree of the regulated output, and it applies to systems that are fully nonlinear with respect to both the states and control (non-affine systems). This error-observer approach allows for high-bandwidth design, and it is this approach that is evaluated in this paper.

Figure 1 presents a block diagram depicting the error observer output feedback adaptive control architecture employed. Uniform ultimate boundedness of all the error signals in the loop has been shown through Lyapunov-like stability analysis. Two forms for the linear controller have been evaluated: (1) Proportional plus Derivative (PD), and (2) Proportional, Integral and Derivative (PID). Details regarding design of the observer, design of the PD compensator, and the design of the adaptive law used to train the neural network weights, as well as the application of the method to attitude control of an unmanned helicopter are presented in Reference 4.

Alternate Design Using PID Compensator

Tests in both simulation and flight indicate that trim variation as a function of flight condition can result in steady state errors that are not compensated by

the neural network. For this reason, integral action has been introduced into the design documented in Reference 4 by employing a PID rather than PD structure for the linear compensator. In this case, $H(s)$ of Figure 1, which for the PD design was given as

$$H(s) = K_D s + K_P \quad (1)$$

is modified to

$$H(s) = \frac{K_D s^2 + K_P s + K_I}{s} \quad (2)$$

In the later case, we prefer to invert a system that has one pole at the origin and two shifted poles. That is a system of the form

$$G(s) = \frac{p^2}{s(s+p)^2} \quad (3)$$

We then seek a design in which two closed-loop poles are attracted to the zero, leaving one dominant second order mode.

Pseudo Control Hedging

Essential to the design of the high-bandwidth attitude command system described above is the incorporation of pseudo control hedging. This technique is detailed in References 2 and 3. This method enables continued adaptation while the plant input is saturated. Computation of the hedge signal in this case is given by

$$v_{hedge} = \hat{f}(x, \delta_c) - \hat{f}(x, \hat{\delta}_c) \quad (4)$$

Equation (4) represents the difference between the response of the dynamic system model used for inversion that is driven directly by the model inversion output, and the response of that same model when driven by the model inversion output subjected to control system authority limits, actuator command quantization, actuator command transport delay, modeled actuator dynamics, as well as actuator endpoints and rate limits. Figure 2 presents a detailed block diagram of the hedge estimation process for the testbed helicopter.

Unmanned Helicopter Testbed

A facility for simulating and flight testing advanced adaptive control algorithms on unmanned

helicopters has been evolved jointly by the Georgia Institute of Technology and Guided Systems Technologies, Inc (GST). This facility was used to generate the numerical results presented in later sections, and is described in the following.

Flight Vehicle and Ground Station

The current generation test bed is based on the airframe of the Yamaha Model R50 production unmanned helicopter⁵. It features a roughly ten foot diameter rotor driven by a twelve horsepower liquid cooled engine, and has an approximate useful payload of forty-four pounds. The helicopter has been outfitted with a general-purpose aluminum enclosure located underneath the fuselage. This enclosure houses the experimental control system avionics and is pictured in Figure 3.

The flight vehicle is supported by a PC-based ground station. Communication between flight control and ground station computers is maintained using a two-way digital radio link. This link is used to transmit GPS differential corrections, operator commands, and various control system configuration parameters to the vehicle, and to obtain from the vehicle data on system operation during flight. A safety pilot is employed at all times. The safety pilot is outfitted with an independent hand-held radio transmitter. With the flip of a switch, he can bypass the flight control computer and pilot the helicopter directly by line of sight⁵.

Flight Control System Implementation

The control system formulation referenced in the previous sections has been coded in the C programming language. It runs in real-time in double precision with a nominal update rate of 100 Hertz on a 200 MHz Pentium-based single board computer. Select components of the attitude command system (the neural network update laws, the filters at the inputs to the neural networks and the actuator dynamic models used for hedging) are updated at 200 Hz. The computer employs a custom real-time operating system. The sensor suite consists of a tactical-grade GPS-aided inertial navigation solution, augmented with a 3-axis magnetometer for heading initialization and ultrasonic ranging for precision geometric altitude measurement during take-off and landing⁵.

Real-Time Hardware-in-the-Loop Simulation

A nonlinear simulation model of the test bed helicopter has been developed for controller validation and software testing based on the math model given in

Reference 6. It includes a six degrees-of-freedom fuselage rigid body model, as well as a first-order representation of main rotor flapping and quasi-steady representations of main and tail rotor inflows. The simulation also includes the simple control rotor model developed in Reference 7, models of first order actuator dynamics, control linkages and limits, sensor noise, bias and latency, transport delays, and simple engine and rotor RPM dynamics. The model has been validated against flight test data for a few key parameters⁸. It is simple enough to run in real-time on a typical desktop PC, and is coupled to the real-time flight control system to produce a hardware-in-the-loop simulation capability. Response of the actuators is presently simulated, not measured. In this form, the utility of the real-time simulation is primarily software test and validation. All of the simulation numerical results presented in the next section were generated on the flight system hardware using the control system software that has been prepared for flight evaluation. All results include actuator, rotor and sensor models, noise, system time delays, and gust inputs.

Numerical Simulation and Flight Test Results

Error Observer Design with PD Compensator

Figure 4 presents a time history of the pitch axis attitude response of the test bed helicopter collected in flight near hover for a design natural frequency of 4.5 radians per second. All of the results presented hereafter are for flight near hover unless indicated otherwise. The vertical axis represents a peak-to-peak attitude range of plus and minus 30 degrees unless indicated otherwise. The horizontal axis is time in seconds, with a typical duration of 25 seconds. This result employs the error observer design using a PD controller. There are three traces shown. The remote pilot generated pitch attitude command is presented in green, and the measured pitch attitude response is presented in orange. The neural network (NN) contribution to the control is plotted in red and is very nearly zero throughout. The colored bars underneath the plot indicate that the neural network was disabled midway through the data collection process in order to illustrate its contribution to the tracking performance. Good tracking of the commands is illustrated, and tracking is improved when using the neural network.

Figure 5 presents two similar time histories from flight test. In the upper plot of Figure 5, the design natural frequency is 4.5 as in Figure 4, but the command is now a computer generated “square” wave.

Tracking of this type of command as the design bandwidth is increased typically results in extended periods of actuator position and rate saturation. The NN is turned off at the midpoint of the trace to illustrate its contribution to tracking performance. In the lower plot, the NN is on all the time. The design natural frequency is raised from 4.5 to 5.5 at the midpoint. Excessive distortion of the command results from the hedging of actuator rate and position limits, so the design frequency is reduced back to 4.5.

In all of the results presented thus far, an optimistic 0.01 seconds of system time delay was included in the hedge calculation. The exact amount of time delay present in the electronic system implementation is not known at this time. The nonlinear simulation was used to study the sensitivity of the flight system to system time delays. In Figure 6 we see the simulated response of the flight system in the presence of 0.03 seconds of pure time delay. Tracking at the design natural frequency of 4.5 radians per second with only 0.01 seconds of time delay hedged (shown on the far left) is good, but degrades severely when the design bandwidth is raised to 7.0 radians per second. Midway across the plot the amount of time delay being hedged is increased to 0.06 seconds. The squared wave command, previously distorted by the hedging of position and rate saturation, is recovered, and tracking of the command is reasonable. The neural network is disengaged for a short period, and then engaged again, on the far right to illustrate its contribution to control. However, this result was not confirmed in flight test. Rather, in the tests conducted to date, hedging of additional time delay in flight did not prevent oscillations at design natural frequencies above 5.5 radians per second.

Just prior to preparation of this publication, it was determined that alternate choices for the parameters employed in the hedge signal calculation (in particular the time constant assumed for the actuator) produced good behavior of the high bandwidth designs in the presence of the time delays shown without experiencing oscillations in the hedged command and the response. Initial flight tests confirmed this result.

Figure 7 presents a representative flight test result for the case of design natural frequency set at 8.0 radians per second. The NN is on at all times, and its output (shown in red) has been greatly amplified relative to those previously shown by the plotting routine used during the test, not by the increase in design natural frequency. Good tracking of the commands is evident, though there is significant distortion of the commands due to hedging. Flight at 9.0 radians per second was similar, and it is anticipated

that further adjustment of the hedging parameters will reduce distortion of the square wave command. The pitch actuator is position or rate saturated almost continuously during this test sequence. This result illustrates the potential to use the developed method to design very high bandwidth nonlinear adaptive controllers that are subject to the presence of unmodeled dynamics in the bandwidth of the controller (the control rotor in this case), significant time delays, and sustained periods of control saturation.

Error Observer Design with PID Compensator

The alternate PID design reported in the previous section was implemented in the nonlinear real-time hardware-in-the-loop simulation facility and evaluated for a design natural frequency over the range from 3.0 to 10.0 radians per second. As in the case of the PD design, good tracking performance was obtained without excessive hedging of the command signal at up to 10.0 radians per second in the presence of actuator dynamics, unmodeled control rotor and main rotor dynamics, system time delays, sensor bias, noise and latency, and wind gusts. Figure 8 presents a sample time history of the simulated pitch channel response at a design natural frequency of 9.0 radians per second for the case in which a nose down pitch command is superimposed on the normal square wave command. The helicopter rapidly transitions to high speed forward flight. The model being inverted for control however, is for hover only. The trim error that results is readily compensated by the added integral action, thus good tracking of the attitude command is maintained across the forward flight regime.

Figure 9 presents a preliminary pitch channel flight test result for the PID formulation of the error observer design. The design natural frequency is set to 4.0 radians per second. Good tracking of the pilot generated commands is evident. Additional flight testing is planned in which the bandwidth of the PID formulation will be raised.

Summary and Conclusions

Both PD and PID variations of an output feedback formulation of a nonlinear adaptive attitude command system for an unmanned helicopter have been tested. The PD form produces excellent results in nonlinear simulation for design natural frequencies up to 10 radians per second. Very good correlation between simulation and flight test for the PD design is obtained to just over 5.0 radians per second. Oscillations that occur in flight test above 5.0 radians per second are reproduced in simulation by adding pure

time delay to the simulation model, and can be compensated in the simulation by either hedging additional time delay, or modifying the actuator model time constant used in construction of the hedge signal. Hedging of additional time delay in flight test did not produce a significant improvement, however altering the actuator model time constant used for hedging allowed for flight at up to 9.0 radians per second. It is anticipated that further tuning of the design parameters used in the hedge calculation will result in further improvements to the demonstrated performance of the system.

The PD form with NN does not fully compensate for trim variation with flight speed. A PID formulation has been developed to address the resulting steady-state error. The PID formulation was tested in nonlinear simulation and provided excellent results up to a design natural frequency of 10 radians per second. Preliminary tests of the PID formulation have demonstrated flight operation up to a design natural frequency of 4.0 radians per second.

Acknowledgements

This work was supported in part by the U.S. Army Research Office under Contract NCC 2-945. The authors would like to acknowledge the contributions of Georgia Tech Post Doctoral Researcher Dr. Naira Hovakimyan, as well as those of the many Georgia Tech graduate students who have contributed to the generation of these results.

References

- ¹Calise, A. J., Prasad, J.V.R., and Corban, J. E., Flight Evaluation of an Adaptive Neural Network Flight Controller of an Uninhabited Helicopter. Paper No P6, *Twenty-Fifth European Rotorcraft Forum*, September 14-16, 1999, Rome, Italy.
- ²Calise, A.J., Lee, Hungu, and Kim, Nakwan, "High Bandwidth Adaptive Flight Control," *AIAA Guidance, Navigation, and Control Conference*, 2000.
- ³Corban, J.E., A.J. Calise and J.V.R. Prasad, "Flight Test of an Adaptive Control System for Unmanned Helicopter Trajectory Following," *AIAA Guidance, Navigation, and Control Conference*, 2000, AIAA-2000-4058.
- ⁴Hovakimyan, N., N. Kim, A. J. Calise, J.V.R. Prasad and J. E. Corban, "Adaptive Output Feedback for High-Bandwidth Control of an Unmanned Helicopter," *AIAA Guidance, Navigation, and Control Conference*, 2001.

⁵J.E. Corban, A.J. Calise, and J.V.R. Prasad, "Implementation of Adaptive Nonlinear Control for Flight Test on an Unmanned Helicopter", Proceedings on the 37th IEEE Conference on Decision & Control, 1998.

⁶Heffley, R. K., M. A. Mních, "Minimum-Complexity Helicopter Simulation Model Math Model, NASA CR-177476, USAAVSCOM Technical Report 87-A-7, April 1988.

⁷Perhinschi, M. and Prasad, J.V.R., "A Simulation

Model of an Autonomous Helicopter," Proceedings of the RPV/UAV Systems 13th Digital International Conference, April 1998.

⁸Munzinger, Christian, "Development of a Real-Time Flight Simulator for and Experimental Model Helicopter," Diploma Thesis, December 1998, Georgia Institute of Technology/University of Stuttgart.

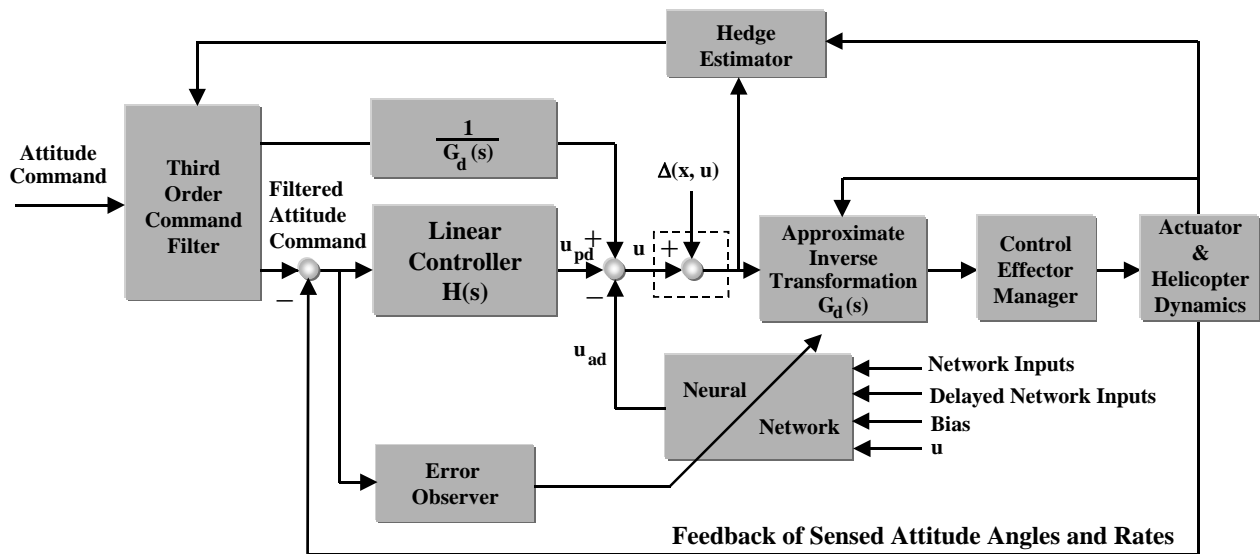


Figure 1. Neural Network Adaptive Output Feedback Attitude Command System employing Error Observer.

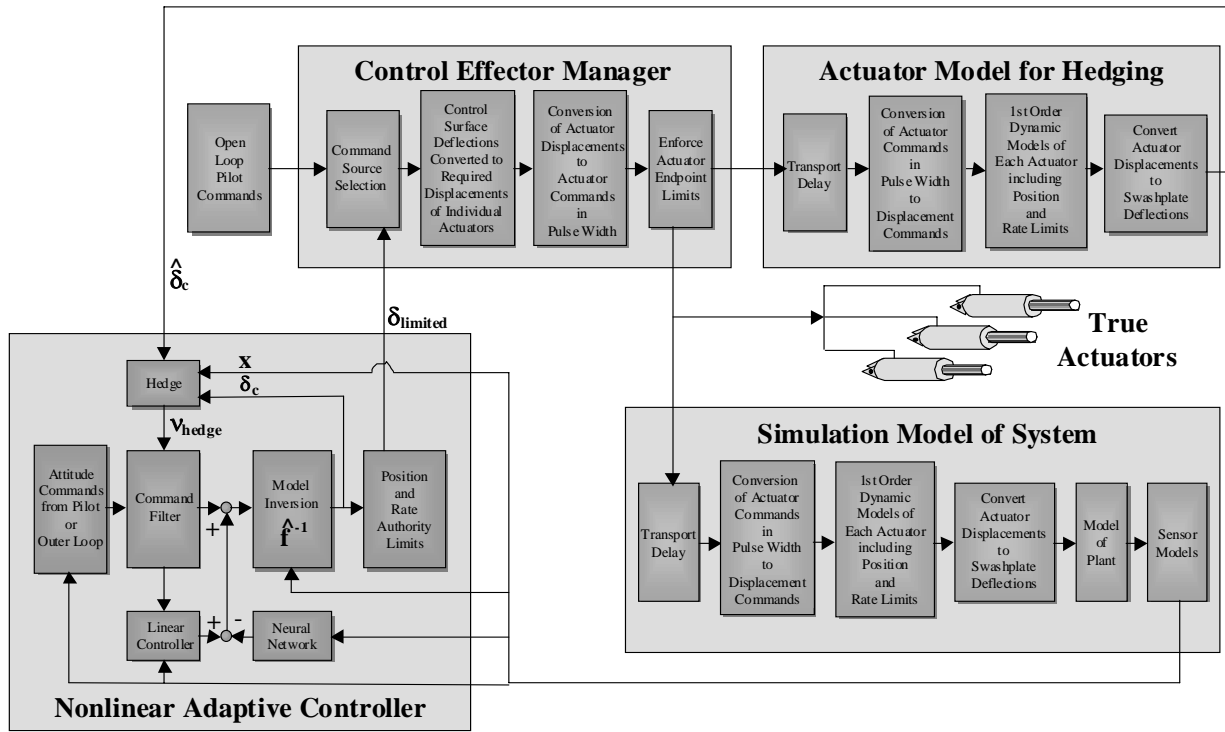


Figure 2. Block diagram depicting implementation of pseudo control hedging for control system authority limits, actuator command quantization, actuator dynamics, actuator position and rate limits, and actuator command transport delay.



Figure 3. Joint Unmanned Helicopter Control Systems Testbed.

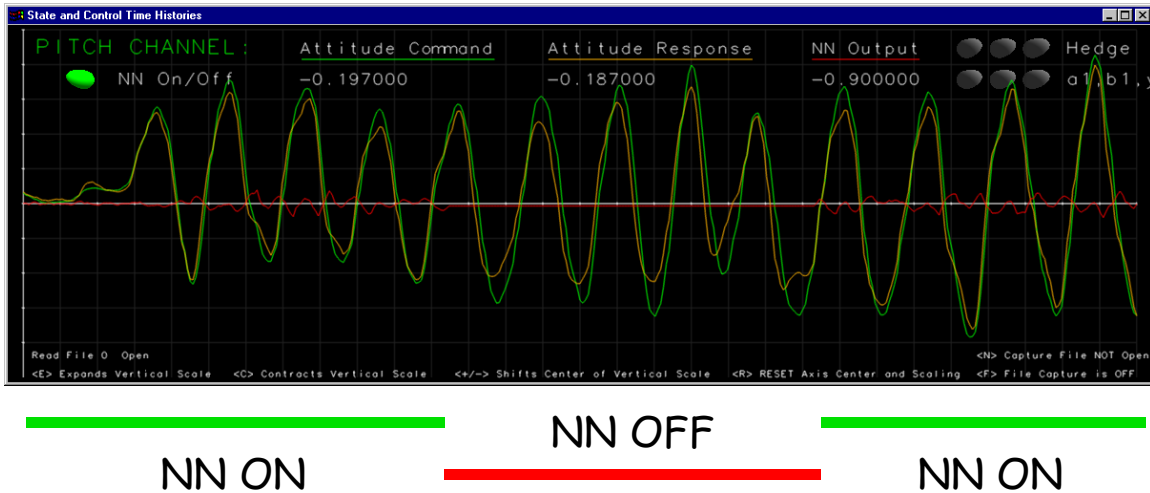


Figure 4. Pitch Channel Flight Test Time History. Design Natural Frequency is 4.5 radians per second using the Error Observer Approach with PD controller.

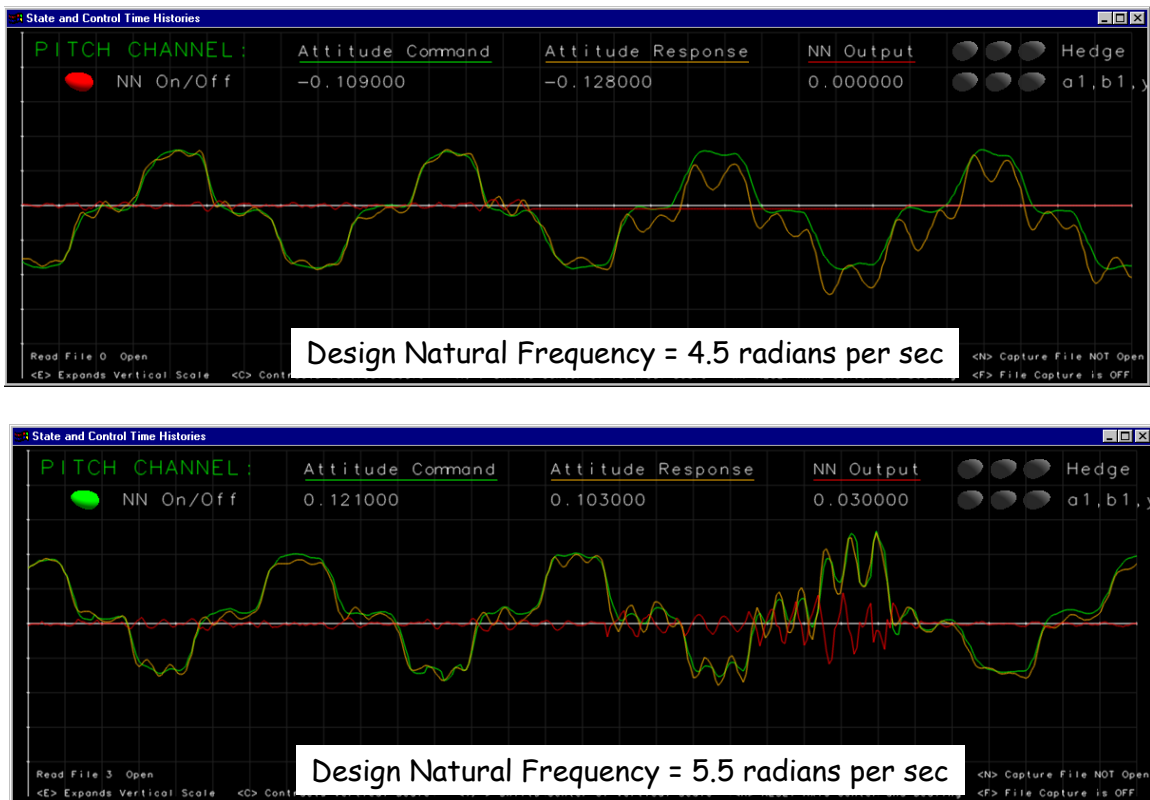
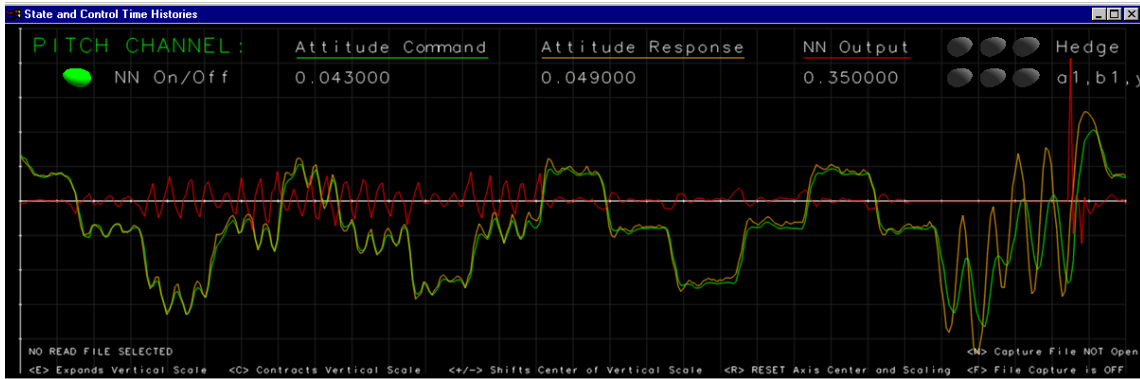


Figure 5. Pitch Channel Flight Test Time History for Square Wave Input using the Error Observer Approach with PD controller. In the upper plot, the design natural frequency is 4.5, and the NN is turned off at the midpoint to illustrate its contribution to tracking performance. In the lower plot, the NN is on all the time, and the design natural frequency is raised from 4.5 to 5.5 at the midpoint. Severe distortion of the command results from the hedging of rate and position limits, so the design frequency is reduced back to 4.5.



4.5 rad/sec

7.0 rad/sec

Hedge 1 Cycle of Delay

Hedge 6 Cycles of Delay

NN OFF

Figure 6. Simulated Pitch Channel Time History for a Square Wave Input using the Error Observer Approach with PD controller. Hedging of additional system time delay is used to improve performance.



Figure 7. Pitch Channel Flight Test Time History for Combined Pilot and Square Wave Input using the Error Observer Approach with PD controller. Design natural frequency is 8.0 radians per second with hedge actuator model time constant reduced from 0.04 to 0.01.

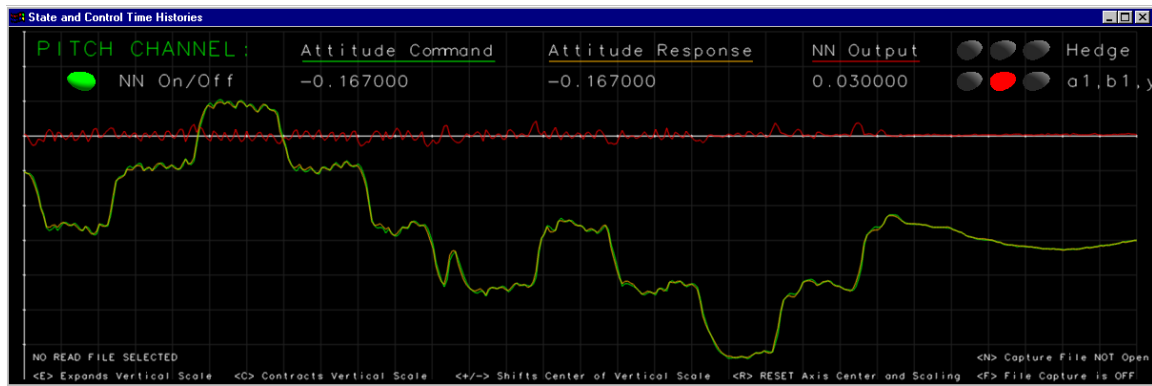


Figure 8. Simulated Pitch Channel Time History with Square Wave Input using the Error Observer Approach with PID controller. Design natural frequency is 10.0 radians per second.

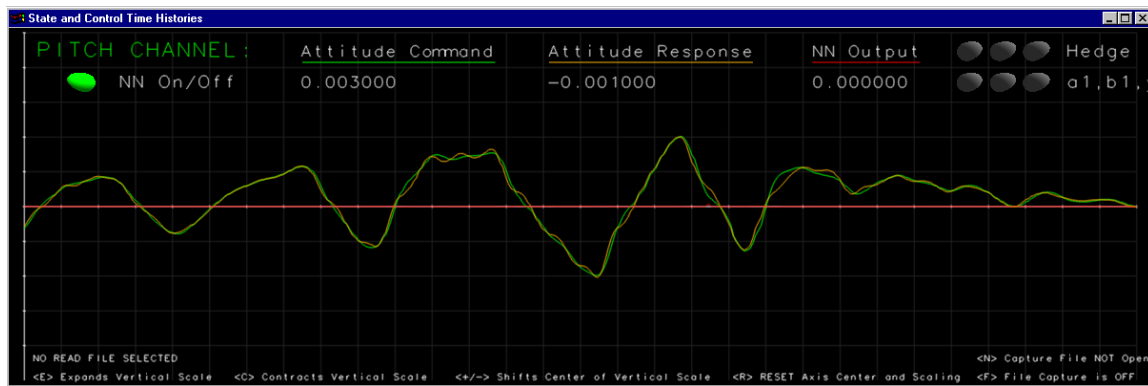


Figure 9. Pitch Channel Flight Test Time History. Tracking of Pilot-Generated Command using the Error Observer Approach with PID controller. Design natural frequency is 4.0 radians per second.